New Correlation for Sieve-Tray Point Efficiency, Entrainment, and Section Efficiency

Douglas L. Bennett
Air Products and Chemicals, Inc., Allentown, PA 18195

Dana N. Watson
Dept. of Chemical Engineering, Purdue University, West Lafayette, IN 47906

Marie Anne Wiescinski
Dept. of Chemical Engineering, University of Michigan, Ann Arbor, MI 48104

A comprehensive composite database for distillation sieve-tray efficiency is used to develop point efficiency and entrainment correlations based on a model that considers the fluid on the distillation tray to be contained in a liquid-continuous region near the tray deck and a vapor-continuous region on top of the liquid-continuous region. This model allows estimates of the portion of the mass transfer that occurs in each region and the mass-transfer resistance that occurs on the liquid side and vapor side of the interface. For most cases, most of the mass transfer occurs within the liquid-continuous region. The liquid side resistance is often significant.

The entrainment correlation is consistent with the work of Bennett et al., which relates entrainment to the ratios of the liquid to vapor density and the froth height to the tray spacing. A simple liquid continuous-only mass-transfer model containing only four empirical parameters correlates the point efficiency data to within 6.4%. Despite a twofold change in vapor Schmidt number, no dependency on vapor Schmidt number is seen. Important dimensionless groupings are the Reynolds number based on the hole velocity, effective froth density, ratio of the liquid inventory to the perforation diameter, and fraction of the tray area perforated. Mathematically simple and accurate methods allow the prediction of the section efficiency for trays operating in cross or parallel flow. They address vapor and liquid mixing, entrainment and a criterion to avoid significant degradation of the tray efficiency due to weeping.

Introduction

Sieve trays continue to be the standard equipment used for distillation columns. Properly designed sieve trays are efficient, low cost, and can be turned down by about a factor of 2. The overall efficiency of a distillation tray requires knowledge of the point efficiency, the random mixing that occurs from the passage of the vapor through the liquid inventory, the velocity pattern on the tray that results from maldistribution of the liquid flowing onto the tray, and the geometry of the tray, the location and amount of weeping or entrainment, and the stripping factor, which is the ratio of the slope of the equilibrium line to the liquid flow to vapor flow ratio. For well-designed trays, the weeping is negligible and the tray diameter is sufficiently large so that the random mixing and the adverse impact of typical velocity patterns has little impact on the overall tray efficiency. For such cases, the overall tray efficiency is largely a function of the stripping factor, the point efficiency, and the entrainment. The stripping factor is controlled by thermodynamic properties and the feed and desired product rates. This article addresses the other two major factors, the point efficiency and the entrainment.

As the vapor passes through the liquid inventory, a mixture of these two phases occurs, forming a biphase. The structure

Correspondence concerning this article should be addressed to D. L. Bennett.

of the biphase has often been assumed to be either spraylike (vapor continuous) or frothlike (liquid continuous). Such a distinction requires a criterion to distinguish between these regimes. Previous modeling attempts for point efficiency have typically assumed either a spraylike or a frothlike biphase structure. For our approach we treat the biphase as a combination of a liquid-continuous region located next to the tray deck and a vapor-continuous region located above the liquid-continuous region. This more complex approach allows us to address the mass transfer in each region, treating the mass transfer as a continuum as we move from a mostly spraylike to a mostly frothlike structure.

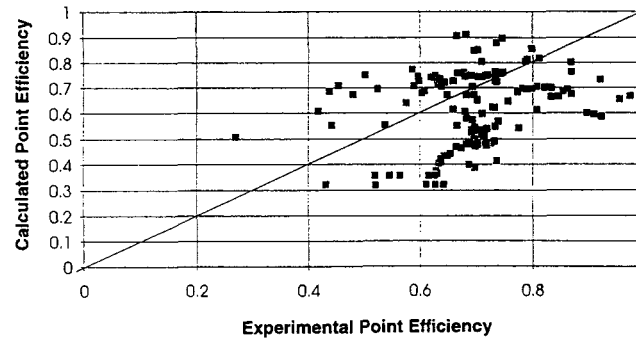

Figure 1. Parity of experimental point efficiency vs. the Chan and Fair point-efficiency correlation.

Background

One of the first correlations for point efficiency was published by AIChE (1958). The experimental absorption and stripping data were developed for bubble-cap trays, yet have been applied to sieve trays. We designate this correlation the AIChE method. It is based on a two-resistance film model for the mass transfer. Vapor-phase and liquid-phase mass transfer are expressed in terms of transfer units for each resistance. Correlations are proposed for the number of transfer units for each resistance as a function of operating conditions and tray geometry. The AIChE method correlations for the number of transfer units are simple curve fits against basic operating and geometry parameters. The very highly empirical nature of this technique questions its applicability to the wide range of operating conditions and properties typical of distillation-tray design. Large errors are reported for the AIChE method by many authors, including Hughmark (1965), Chan and Fair (1984), and Biddulph and Dribika (1986).

Hughmark (1965) uses the AIChE study data and develops correlations for the transfer units based on Higbie's penetration theory. Hughmark observes that the AIChE method gives poor results when the liquid-phase resistance dominates. Hughmark bases his froth-height correlation on Soulders and Brown (1934) density-corrected velocity instead of the F-factor ($\sqrt{\rho_V} V_B$) and weir height as was done in the AIChE method. The clear-liquid height correlation was not adjusted. When high liquid phase resistance occurred, Hughmark's correlation decreases the deviation to 16.5% as compared to 38.7%, which he calculates with the AIChE method.

Zuiderweg (1982) uses commercial sieve tray data, acquired from FRI, and applies the slope and intercept method to develop expressions for the mass-transfer coefficients. Zuiderweg develops separate expressions for both spray and froth for the two-phase density, axial mixing, liquid entrainment, lower operating limit, and interfacial area. Separate sets of equations for each regime is burdensome and still does not give a marked increase in accuracy.

The Chan and Fair (1984) correlation is often used to estimate the point efficiency. Their correlation for the number of liquid-phase transfer units is identical to the AIChE method. They developed a new expression for the number of vapor-phase transfer units. They considered tray loading, and therefore indirectly considered entrainment by introducing a correlating parameter *ff*, which is the ratio of the superficial velocity to that which would result in flooding. The value for this factor is obtained by Chan and Fair for each data set from either reported values for flooding or, when not stated, the highest gas throughput when accompanied by significant entrainment. Using the reported value for each data set, an average error of 6.27% was obtained. The authors also acknowledge that the "flood point as used here is not the true flood condition indicated by very low efficiency."

Chan and Fair do not offer a calculation method to estimate *ff*. To independently estimate the flood point, as would be required by a user without the benefit of tests, we have used the empirical fit of the Fair (1961) sieve-tray flooding correlation reported by Treybal (1968). For our composite database, this flooding correlation can calculate values for *ff* that are greater than unity or even values that are negative. We assumed that if the calculated value for *ff* exceeded one, it equaled one. The results from this are illustrated in Figure 1. The average error is 24%. The AIChE method gave 22.9% average error for the Chan and Fair database.

Prado and Fair (1990) present a very interesting study of both flow regimes and mass-transfer modeling. They treat the bi-phase as three regions: a region near the perforations where the gas can be either jetting or bubbling, a bulk froth zone that is composed of gas bubbles dispersed in the liquid and then a spray region. They developed detailed mass-transfer models and expressions for each region. Many of the empirical correlations are restricted to air/water.

In summary, most existing correlations for point efficiency are highly empirical and based on only the simplest modeling of the bi-phase. The Chan and Fair (1984) correlation was developed using an extensive database and is recommended widely. The lack of an acceptable correlation for the parameter *ff* makes their correlation difficult to use when accurate point efficiencies are required. The success of other existing general correlations, for example, the AIChE method, has been inadequate for the reliable design of sieve-tray columns.

Composite Database

We have based our correlation on larger-scale tray data where realistic phenomena such as entrainment and weeping may occur. Chan and Fair (1984) also selected this approach and our database is nearly the same as used by them. Our database consists of Jones and Pyle's (1955) acetic acid/water system data, Nutter's (1972) ammonia stripping data, Sakata and Yanagi's (1979) cyclohexane/*n*-heptane and isobutane/*n*-butane data, and Yanagi and Sakata's (1982) cyclohexane/*n*-heptane and isobutane/*n*-butane data. The data

Table 1. Geometry and Operating Ranges

Parameter	Minimum	Average	Maximum	Max/Min
Perforation dia. (m)	0.0032	0.009	0.0127	4
Tray spacing (m)	0.30	0.54	0.61	2
Weir height (m)	0.038	0.046	0.051	1.3
A_H/A_B	0.08	0.10	0.14	1.74
L/V	0.90	2.54	18.3	20
Slope of equil. line	0.633	0.861	1.139	1.8
$m/(L/V)$	0.043	0.725	1.13	26
Vapor rate, K_S (m/s)	0.01	0.068	0.15	15
Liquid rate (m^3/s/m)	0.00015	0.00505	0.0212	140
Liquid inventory (m)	0.0076	0.027	0.066	8.7
No. of mixing cells	1.02	2.62	10.43	10

were all for binary separations and taken with single-pass cross-flow trays.

The entire database consisted of 156 data sets. Tables 1 and 2 show that the composite database covers a wide range of geometry, operating conditions, and a wide range for the values of the dimensionless groupings.

Method to calculate the point efficiency

We have assumed for each of these data sets that within the column section the operating line, L/V, the slope of the equilibrium line, m, and the Murphree efficiency are constant. Under these conditions the section efficiency, η_{SECT}, and the Murphree efficiency, η_{MV}, are related by

$$\eta_{SECT} = \frac{\ln(1+\eta_{MV}(\lambda-1))}{\ln \lambda}, \tag{1}$$

where $\lambda = m/(L/V)$.

The point efficiency is then calculated from the Murphree efficiency. Since the data are taken with large-size trays under wide operating conditions, entrainment of liquid is sometimes significant. The Murphree efficiency is a function of both the point efficiency and the entrainment. Bennett et al. (1995) gave an empirical expression based on numerical results that gives the impact of entrainment recirculation on Murphree efficiency. Their equation is

$$\frac{\eta_{MV}(E)}{\eta_{MV}(E=0)} = 1 - 0.8\eta_{PT}\lambda^{0.543}E\frac{V}{L}, \tag{2}$$

where E is the ratio of the mass flux of entrainment to the mass flux of vapor through the tray, $\eta_{MV}(E)$ and $\eta_{MV}(E=0)$ are the Murphree efficiency values with entrainment and the value if there was no entrainment. We will discuss later how we estimate entrainment.

Table 2. Range of Dimensionless Groupings

Parameter	Minimum	Average	Maximum	Max/Min
Re_{DH}	970	34,000	180,000	180
$Re_{h_{Fe}}$	12,000	290,000	2,200,000	180
Re_{Liquid}	9,200	38,000	69,700	7.6
We_{DH}	1.18	250	1,550	1,300
We_{DB}	1.95	145	1,070	550
Sc_{Liq}	3.09	195	920	300
Sc_{Vap}	0.75	1.17	1.70	2.3
$(\rho_L - \rho_V)/\rho_V$	2.37	745	1465	620
h_{Fe}/D_H	4.45	10.0	24.1	5.4
h_L/D_H	1.30	3.43	9.20	7.06
$h_{Fe}/h_{2\phi}$	0.024	0.370	0.97	39
$h_{2\phi}/T_S$	0.097	1.27	6.80	70

The point efficiency and the Murphree efficiency with no entrainment are still unknown and related through the definitions of the efficiencies and the conservation of mass on a tray. The conservation of mass equations and associated boundary conditions are based on the flow direction, for example, parallel or crossflow, and the assumed mixing within the vapor space above the tray and within the liquid on the tray.

Chan and Fair (1984) assumed that the vapor was well mixed when they calculated the point efficiency. The work of Katayama and Imoto (1972) suggests that for most of the data the vapor is unmixed. To estimate the liquid back-mixing within the bi-phase, we used the correlation for eddy dispersion proposed by Bennett and Grimm (1991) multiplied by four. Since they were only interested in the liquid mixing caused by vapor flowing through the tray, Bennett and Grimm used eddy dispersion data taken only with rectangular trays. For commercial trays the total mixing results from both the vapor flowing through the tray and nonideal flow patterns resulting from the nonuniformity of the inlet flow and the streamline curvature associated with the column shell and the fluid approaching the exit weir. Our experience has shown that the overall liquid mixing on a real tray is better modeled if we use the multiplier of four. This correction is important in cases where point-efficiency data are taken in trays that are neither well mixed nor plug flow. This is true for much of our database, and we have used this correction for this study. The correction for commercial columns is typically unimportant since, even with these nonideal increases in back-mixing, most commercial trays approach the solution for liquid plug flow.

Since the adjusted liquid-phase Peclet number for the data sets ranges from about 0 to about 20 and the vapor mixing can be assumed as unmixed, the appropriate solution for these conditions are those attributable to Diener (1967). The Diener calculation is numerically complex and not easy to use.

An alternate approach is the mixing-pool model attributable to Gautreaux and O'Connell (1955). This model assumes that the vapor is well mixed, which is not valid for our database, but does allow for partial mixing of the liquid. When the vapor is well mixed but the liquid is partially mixed we have verified that the numerical solution for these boundary conditions, for the ranges of $0.5 \le \lambda \le 3.0$, $0.4 \le \eta_{PT} \le 1.0$ and $0 \le Pe_L \le 1{,}000$, can be approximated to within an average error of $\pm 0.4\%$ if we calculate the Murphree efficiency from the mixing-pool model by

$$\eta_{MV_{\text{vapor-mixed}}} = \frac{[1+(\lambda\eta_{PT}/N)]^N - 1}{\lambda}, \tag{3a}$$

where N is the number of mixing cells on the tray and is dependent on the liquid Peclet number, Pe_L, by

$$N = \frac{Pe_L + 2}{2} \tag{3b}$$

In this model, since the vapor is assumed to be mixed prior to entering the tray above, there is no dependency of the Murphree efficiency on the liquid flow direction (parallel or crossflow). When the vapor is unmixed the Murphree efficiency is dependent on the flow direction. For parallel flow and unmixed vapor we have found that the Diener solution, for the ranges of $0.5 \le \lambda \le 3.0$, $0.4 \le \eta_{PT} \le 1.0$ and $0 \le Pe_L \le 1{,}000$, can be approximated to within an average error of $\pm 1.5\%$ by

$$\eta_{MV_{\text{Parallel, unmixed - vapor}}} = \frac{[1+(\lambda\eta_{PT}/N)]^N - 1}{\lambda} \times [1 + 0.0463\lambda^{0.6255}\eta_{PT}^{1.69591}Pe_L^{0.16625}]. \quad (4a)$$

For the cross-flow case with vapor unmixed, the Diener solution for the ranges of $0.5 \le \lambda \le 3.0$, $0.4 \le \eta_{PT} \le 1.0$, and $0 \le Pe_L \le 1{,}000$ can be approximated to within an average error of $\pm 1.5\%$ by

$$\eta_{MV_{\text{Cross-flow, unmixed - vapor}}} = \frac{[1+(\lambda\eta_{PT}/N)]^N - 1}{\lambda} \times [1 - 0.0335\lambda^{1.07272}\eta_{PT}^{2.51844}Pe_L^{0.17524}]. \quad (4b)$$

All of the data within our composite database was taken with cross-flow trays. We will be using Eq. 4b for data reduction.

Just because entrainment clearly impacts the section and Murphree efficiency due to recirculation of liquid, does it also impact the point efficiency? For most cases, the point efficiency is not significantly impacted by the presence of the tray above since almost all of the mass transfer occurs nearer to the tray deck. We will reexamine this assumption later, but for now we assume that the point efficiency is independent of the entrainment.

When entrainment is small or near zero, Eqs. 1 and 4b can be used to calculate the point efficiency. When entrainment is important, we will use Eq. 1 to calculate the Murphree efficiency, estimate entrainment, and then determine the Murphree efficiency for the no-entrainment case, using Eq. 2. This value of the Murphree efficiency, adjusted to the no-entrainment value, is then used in Eq. 4b to determine the point efficiency.

Phenomenological Model for Point Efficiency

Biphase structure and definitions of efficiency

We have used the two-zone model illustrated in Figure 2. This model has a liquid-continuous region located near the tray deck and a vapor-continuous region above the liquid-continuous region.

The liquid-continuous region of the biphase has a height, h_{LC}, and an average froth density, ϕ_{LC}. The vapor-continuous region has a height, h_{VC}, and an average froth density, ϕ_{VC}. A mass balance gives

$$h_L = \phi_e h_{Fe} = \phi_{2\phi} h_{2\phi} = \phi_{LC} h_{LC} + \phi_{VC} h_{VC},$$

where the total liquid inventory on the tray is h_L; ϕ_e and h_{Fe} are the effective froth density and effective froth height as defined by Bennett et al. (1983); and $\phi_{2\phi}$ and $h_{2\phi}$ are the average froth density and total froth height of the entire biphase.

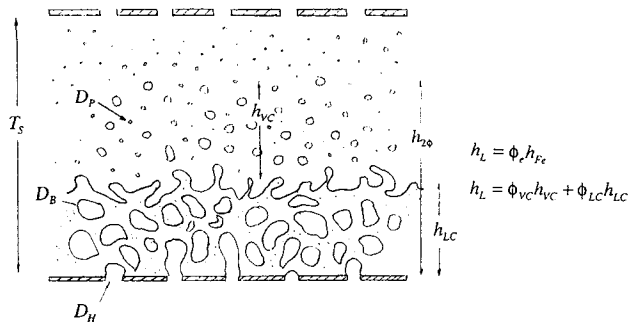

Figure 2. Depiction of the two-zone model.

We define f as the ratio of the total mass within the vapor-continuous region to the total liquid inventory;

$$\frac{\phi_{VC}(h_{2\phi} - h_{LC})}{\phi_e h_{Fe}} = f.$$

This allows us to solve for the average froth density in both the vapor- and the liquid-continuous regions:

$$\phi_{VC} = \frac{\phi_e h_{Fe}}{(h_{2\phi} - h_{LC})} f \quad (5a)$$

$$\phi_{LC} = \phi_e \frac{h_{Fe}}{h_{LC}}(1-f). \quad (5b)$$

The actual relationship for f will be addressed later, but values are expected to approach zero as h_L/D_H becomes large when almost all the mass within the bi-phase is contained in the liquid-continuous region.

We will use the conventional assumption of well-mixed liquid in the vertical direction throughout the entire biphase. The expression for the point efficiency for the liquid-continuous region, $\eta_{PT_{LC}}$, is

$$\eta_{PT_{LC}} = \frac{y(0) - y(h_{LC})}{y(0) - y^*(x)}, \quad (6a)$$

where the mole fraction of the vapor as it enters the tray is $y(0)$, and at the top of the liquid-continuous region it is $y(h_{LC})$; $y^*(x)$ is the composition of the vapor if it were in equilibrium with the liquid composition, x.

The corresponding definition for the point efficiency for the vapor-continuous region, $\eta_{PT_{VC}}$, is

$$\eta_{PT_{VC}} = \frac{y(h_{LC}) - y(h_{2\phi})}{y(h_{LC}) - y^*(x)}, \quad (6b)$$

where the vapor mole fraction at the top of the biphase is $y(h_{2\phi})$.

The overall point efficiency is

$$\eta_{PT} = \frac{y(0) - y(h_{2\phi})}{y(0) - y^*(x)} \tag{6c}$$

These three expressions can be combined to yield

$$\eta_{PT} = \eta_{PT_{VC}} + \eta_{PT_{LC}}(1 - \eta_{PT_{VC}}). \tag{6d}$$

Dividing Eq. 6a by Eq. 6c shows that the ratio $\eta_{PT_{LC}}/\eta_{PT}$ is equal to the ratio of the change in the composition of vapor within the liquid-continuous region to the total bi-phase change in vapor composition. Therefore, $\eta_{PT_{LC}}/\eta_{PT}$ is the fraction of the total mass transfer that occurs within the liquid-continuous region.

Application of the two-film model

For either the liquid-continuous or vapor-continuous region, the gas-phase mass-transfer coefficient, k_G, and the liquid-phase mass-transfer coefficient, k_L, can be defined by

$$N_A = \rho_{M_V} k_G A(y - y_i) = \rho_{M_L} k_L A(x_i - x),$$

where ρ_{M_V} and ρ_{M_L} are the mole density of the vapor and the liquid; A is the area across which the mass transfer is occurring; and the subscript i indicates the composition at the interface, while x and y are the bulk mole fractions in the liquid and vapor phase.

Assuming that the liquid and vapor are in equilibrium at the interface, the local slope of the equilibrium line, m, can be defined as $y_i = mx_i + b$, where b in this case is the y-axis intercept. The expressions just given can be combined to eliminate the need to know the interface compositions and to express the mass transfer in terms of the overall driving force:

$$N_A = \frac{1}{\frac{1}{k_G} + \frac{\rho_{M_V} m}{\rho_{M_L} k_L}} \rho_{M_V} A[y - y^*(x)]$$

$$= K_{OG} \rho_{M_V} A[y - y^*(x)], \tag{7}$$

and K_{OG} is the overall gas-phase mass-transfer coefficient within the region.

Equation 7 is valid for both the liquid-continuous and vapor-continuous regions. The interfacial area and the mass-transfer coefficients k_G and k_L will be different for each region. We will assume that there is a characteristic bubble size within the liquid-continuous region, D_B, and a characteristic droplet size within the vapor-continuous region, D_P. To estimate the height of the liquid-continuous region, we will assume that $h_{LC} = h_{Fe}$, the effective froth height, as defined by Bennett et al. (1983).

The result of a mass balance, integration, and rearrangement gives the following:

$$\eta_{PT_{VC}} = 1 - \exp\frac{-6K_{OG_{VC}}}{K_S}\sqrt{\frac{\rho_V}{\rho_L - \rho_V}}\frac{h_{2\phi} - h_{Fe}}{D_P}\phi_{VC} \tag{8a}$$

$$\eta_{PT_{LC}} = 1 - \exp\frac{-6K_{OG_{LC}}}{K_S}\sqrt{\frac{\rho_V}{\rho_L - \rho_V}}\frac{h_{Fe}}{D_b}(1 - \phi_{LC}), \tag{8b}$$

where, for this two-zone model,

$$\phi_{VC} = \frac{\phi_e h_{Fe}}{(h_{2\phi} - h_{Fe})} f$$

$$\phi_{LC} = \phi_e(1 - f),$$

and K_S is the density-corrected vapor velocity over the bubbling area, V_B

$$K_S = \left(\frac{\rho_V}{\rho_L - \rho_V}\right)^{1/2} V_B.$$

Based on Eq. 7, we can develop expressions for both the overall vapor-continuous ($K_{OG_{VC}}$) and overall liquid-continuous ($K_{OG_{LC}}$) mass transfer coefficients

$$K_{OG_{VC}} = \frac{1}{\frac{1}{k_{G_{VC}}} + \frac{\rho_{M_V} m}{\rho_{M_L} k_{L_{VC}}}} \tag{9a}$$

and

$$K_{OG_{LC}} = \frac{1}{\frac{1}{k_{G_{LC}}} + \frac{\rho_{M_V} m}{\rho_{M_L} k_{L_{LC}}}}. \tag{9b}$$

The Higbie (1935) penetration theory relates mass transfer in a turbulent regime to the transient mass transfer of an infinite fluid element exposed to the interface for a contact time, θ. We will use the Higbie theory to help identify the important dimensionless groupings for each mass-transfer coefficient. This approach yields for the mass-transfer coefficients

$$k_{G_{VC}} = 2\sqrt{\frac{D_G}{\pi\theta_{G_{VC}}}} \tag{9c}$$

$$k_{L_{VC}} = 2\sqrt{\frac{D_L}{\pi\theta_{L_{VC}}}} \tag{9d}$$

$$k_{G_{LC}} = 2\sqrt{\frac{D_G}{\pi\theta_{G_{LC}}}} \tag{9e}$$

$$k_{L_{LC}} = 2\sqrt{\frac{D_L}{\pi\theta_{L_{LC}}}} \tag{9f}$$

where D_G and D_L are the gas-phase and liquid-phase molecular diffusivity, and $\theta_{G_{VC}}$, $\theta_{L_{VC}}$, $\theta_{G_{LC}}$, and $\theta_{L_{LC}}$ are, respectively, the vapor-continuous gas-and liquid-phase contact times and the liquid-continuous gas-and liquid-phase contact times, and π is pi. For the liquid-continuous region,

$$K_{OG_{LC}} = \frac{2\sqrt{\dfrac{D_G}{\pi\theta_{G_{LC}}}}}{1 + m\dfrac{\rho_{M_V}}{\rho_{M_L}}\sqrt{\dfrac{D_G\theta_{L_{LC}}}{D_L\theta_{G_{LC}}}}}. \tag{10a}$$

For the liquid-continuous region we will assume that the contact time for the vapor-side resistance is D_B/V_H, where V_H is the velocity of the vapor through the tray perforation, and the contact time for the liquid-side resistance is D_B/V_{Rise}, where V_{Rise} is the average rise velocity of the bubble and is given by

$$V_{\text{Rise}} = \frac{V_H\left(\dfrac{A_H}{A_B}\right)}{1-\phi_{LC}} = \frac{V_B}{1-\phi_{LC}},$$

where A_H/A_B is the ratio of the perforated area to the total bubbling area.

Equation 10a and these contact times can be combined to give

$$K_{OG_{LC}} = \frac{2\sqrt{\dfrac{D_G V_H}{\pi D_B}}}{1 + m\dfrac{\rho_{M_V}}{\rho_{M_L}}\sqrt{\dfrac{D_G(1-\phi_{LC})}{D_L(A_H/A_B)}}}. \tag{10b}$$

The mass-transfer coefficient, if controlled only by vapor-phase resistance, is determined from Eq. 10b with the assumption that the liquid molecular diffusivity, D_L, equals infinity:

$$K_{OG_{LC}} = 2\sqrt{\frac{D_G V_H}{\pi D_B}},$$

if the liquid-phase resistance is zero. For the liquid-continuous region, the ratio of the overall mass-transfer rate considering liquid- and vapor-side resistance to the mass transfer rate if there is no liquid side resistance, R_{LC}, is

$$R_{LC} = \frac{1}{1 + m\dfrac{\rho_{M_V}}{\rho_{M_L}}\sqrt{\dfrac{D_G(1-\phi_{LC})}{D_L(A_H/A_B)}}}. \tag{10c}$$

Similarly, for the vapor-continuous region,

$$K_{OG_{VC}} = \frac{2\sqrt{\dfrac{D_G}{\pi\theta_{G_{VC}}}}}{1 + m\dfrac{\rho_{M_V}}{\rho_{M_L}}\sqrt{\dfrac{D_G\theta_{L_{VC}}}{D_L\theta_{G_{VC}}}}}.$$

We will assume for the vapor-continuous region that the vapor-side resistance contact time is D_P/V_{ej}, where V_{ej} is the ejection velocity of the droplet as it departs the top of the liquid-continuous region. Since the droplet formation process probably results in all of the liquid contained within the droplet moving at a velocity V_{ej}, the contact time for the liquid-side resistance is approximately the time of flight of the droplet, on order of $(h_{2\phi} - h_{Fe})/V_{ej}$; therefore,

$$K_{OG_{vc}} = \frac{2\sqrt{\dfrac{D_G V_{ej}}{\pi D_P}}}{1 + m\dfrac{\rho_{M_V}}{\rho_{M_L}}\sqrt{\dfrac{D_G}{D_L}\dfrac{(h_{2\phi} - h_{Fe})}{D_P}}}. \tag{10d}$$

We can also develop an expression for the ratio of the overall mass-transfer coefficient in the vapor-continuous region to that which would occur if the liquid-side resistance in the vapor-continuous region were zero. We will call this ratio R_{VC}, and

$$R_{VC} = \frac{1}{1 + m\dfrac{\rho_{M_V}}{\rho_{M_L}}\sqrt{\dfrac{D_G}{D_L}\dfrac{(h_{2\phi} - h_{Fe})}{D_P}}}. \tag{10e}$$

We now have, when we insert Eq. 10d into Eq. 8a,

$$\eta_{PT_{VC}} = 1 - \exp\frac{-12}{K_S\left[1 + m\dfrac{\rho_{M_V}}{\rho_{M_L}}\sqrt{\dfrac{D_G}{D_L}\dfrac{(h_{2\phi} - h_{Fe})}{D_P}}\right] \times \sqrt{\dfrac{D_G V_{ej}}{\pi D_P}\dfrac{\rho_V}{\rho_L - \rho_V}}\dfrac{h_{2\phi} - h_{Fe}}{D_P}\phi_{VC}}. \tag{10f}$$

Selecting the characteristic dimensions: D_B, D_P, h_{Fe}, and $h_{2\phi}$

The bubble diameter from single orifices has been correlated by Kumar et al. (1976). Bennett and Ludwig (1994) give the following curve fit of these results when the Reynolds numbers are between 2,000 and 100,000. Their expression is

$$D_B = 79\left(\frac{\sigma D_H^2}{(\rho_L - \rho_V)\dfrac{g}{g_C}}\right)^{1/4}\left(\frac{\rho_V V_H D_H}{\mu_V}\right)^{-0.38}.$$

In a distillation application, bubbles form in a two-phase froth from multiple orifices. Therefore this relationship may not be valid. We will, however, use this to identify the appropriate dimensionless groupings.

Fair et al. (1984) showed that the maximum droplet size in the spraylike regime can be correlated by a critical Weber number of 15. We are actually interested in the diameter of the average drop, D_P. Even though the average droplet will be smaller, we assume for now that D_P can be calculated from

$$We_{\text{Crit}} = 15 = \frac{\rho_V V_H^2 D_P}{\sigma}.$$

The height of the liquid-continuous region is assumed equal to the effective froth height reported by Bennett et al. (1983), where

$$h_{Fe} = h_W + C\left(\frac{Q_L}{\phi_e}\right)^{2/3},$$

where h_W is the height of the outlet weir (m), Q_L is the volumetric flow rate of liquid per length of weir ($m^3/s/m$), and ϕ_e is the effective froth density:

$$\phi_e = \exp(-12.55K_S^{0.91}),$$

where K_S is the density-corrected vapor velocity expressed in m/s, and C is a constant dependent on the outlet weir height;

$$C = 0.501 + 0.439\exp(-137.8h_W),$$

where the weir height, h_W, is expressed in m.

The overall height of the froth, $h_{2\phi}$, is obtained from Bennett et al. (1995):

$$\frac{h_{2\phi}}{h_{Fe}} = 1 + \left(1 + 6.9\left(\frac{h_L}{D_H}\right)^{-1.85}\right)\frac{Fr_V}{2},$$

where the vapor Froude number, Fr_V is

$$Fr_V = \frac{V_{ej}^2}{gh_{Fe}},$$

where V_{ej} is the ejection velocity of the droplet from the top of the liquid-continuous region and is given by

$$V_{ej} = 3K_S\sqrt{\frac{\sqrt{3}}{(A_H/A_B)\phi_e}}.$$

This correlation calculates the froth height that would result if the tray spacing is greater than the froth height. We will continue to use this expression, even when the calculated froth height exceeds the tray spacing. We have substituted A_H/A_B into the preceding expression instead of using the percent open area of the tray over the perforated region. A_H/A_B is an "apparent" fraction of the tray that is perforated. The original work was carried out with laboratory trays, which typically have perforations up to the edge of the tray. Our data are for real tray designs, which typically have bubbling but nonperforated support regions around the perimeter of the tray. The gas spreads quickly into these nonperforated regions, thereby decreasing the "apparent" fraction of the tray that is perforated. A_H/A_B is typically 10% smaller than the percent open area of the tray over the perforated region. For identical reasons, we have used A_B to calculate K_S from the overall volumetric flow of vapor through the column.

Liquid Continuous-Only Model

We expect, for most of our database, that much of the mass transfer occurs within the liquid-continuous region. If we assume that all of the mass transfer occurs within the liquid-continuous region, $\eta_{PT_{VC}} = 0$, $\phi_{VC} = 0$, and $\phi_{LC} = \phi_e$.

Liquid-continuous-only correlation for a subset of data, ignoring entrainment and weeping

To identify a subset of our database with very little entrainment, consistent with Bennett et al. (1995), we will limit this subset to conditions yielding $h_{2\phi}/T_S \le 0.8$. To avoid data sets where significant weeping might be expected, we will, consistent with Lockett and Banik (1984), exclude data if $Fr_{\text{Liq}} \le 0.5$, where

$$Fr_{\text{Liq}} = \left(\frac{\rho_V V_H^2}{\rho_L g h_L}\right)^{1/2}.$$

Using Eqs. 8b and 10b, we can solve directly for the bubble size from the experimental values of $\eta_{PT_{LC}}$ calculated from the measured section efficiency. The expression is

$$D_B^{3/2} = \frac{-12/\sqrt{\pi}}{1 + m\dfrac{\rho_{M_V}}{\rho_{M_L}}\sqrt{\dfrac{D_G V_H}{D_L V_{\text{Rise}}}}} \frac{h_{Fe}\sqrt{D_G V_H}}{V_{\text{Rise}}\ln(1-\eta_{PT_{LC}})}.$$

For this data subset the typical values back-calculated for D_B are from 5 to 10 mm. The calculated bubble size is larger than we thought reasonable for hydrocarbons, but are surprisingly consistent with those used by Prado and Fair (1990), based on the work of several investigators. The value for R_{LC} for our data subset ranges from 0.95 to 0.50. Since a value of 1.0 would correspond to no liquid-side resistance, these values for R_{LC} indicate that the vapor side resistance is typically controlling the mass-transfer rate. We will eventually take an empirical approach and return to the question of liquid-phase resistance.

We need to estimate the relationship between bubble size and flow parameters and properties. We have assumed, based in part on the work of Kumar et al. (1976), that the structure of the correlation for the bubble size is

$$We_{D_B} = \frac{\rho_V V_H^2 D_B}{g_c \sigma} = f\left(\frac{\rho_V V_H D_H}{\mu_V}, \frac{\rho_L - \rho_V}{\rho_V}\right).$$

Figure 3 illustrates the relationship that we found between the bubble Weber number, using the "experimental" bubble sizes determined with the preceding equation, the Reynolds number, and the relatively complex relationship we found on $(\rho_L - \rho_V)/\rho_V$. We believe that this unusual relationship is a consequence of the rigidity of the Higbie theory. The following functionality, however, seems reasonable;

$$D_B = A\frac{g_c\sigma}{\rho_V V_H^2}\left[\frac{\rho_V V_H D_H}{\mu_V}\right]^B f_1\left[\frac{\rho_L - \rho_V}{\rho_V}\right],$$

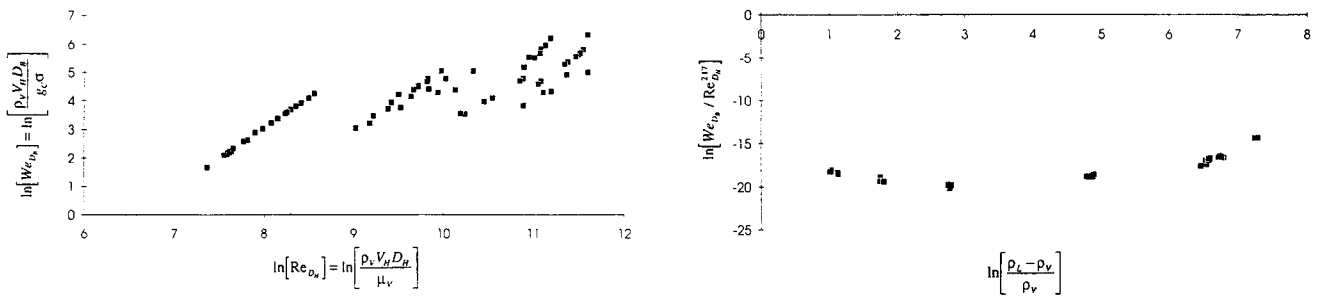

Figure 3. (a) Dependency of bubble Weber number on bubble Reynolds number; (b) dependency of bubble diameter on density ratio.

where A and B are derived constants, and f_1 could be a rather complex relationship of the density ratios.

We can use Eq. 8b to back-calculate what we will call "experimental" values for $K_{OG_{LC}}/D_B$ by using experimental values for $\eta_{PT_{LC}}$:

$$\left[\frac{K_{OG_{LC}}}{D_B}\right]_{\text{exp}} = \frac{-\ln(1-\eta_{PT_{LC}})}{6}\frac{K_S}{h_{Fe}(1-\phi_{LC})}\left(\frac{\rho_L-\rho_V}{\rho_V}\right)^{1/2}.$$

If we can find a successful correlation for these experimental values of $K_{OG_{LC}}/D_B$, we have a correlation for $\eta_{PT_{LC}}$.

Based on Eq. 10b, the functionality we expect for D_B, and the equation for V_{Rise}, we also have

$$\frac{K_{OG_{LC}}}{D_B} = \frac{2/\sqrt{\pi}}{1+m\dfrac{\rho_{M_V}}{\rho_{M_L}}\sqrt{\dfrac{D_G V_H}{D_L V_{\text{Rise}}}}} \times \frac{\sqrt{D_G V_H}}{\left[A\dfrac{g_c\sigma}{\rho_V V_H^2}\left(\dfrac{\rho_V V_H D_H}{\mu_V}\right)^B f_1\left(\dfrac{\rho_L-\rho_V}{\rho_V}\right)\right]^{3/2}}.$$

The preceding two expressions can be equated and variables grouped to yield:

$$\frac{-\ln\left(1-\eta_{PT_{LC_{\text{only}}}}\right)}{6} = \frac{2/\sqrt{\pi}}{1+m\dfrac{\rho_{M_V}}{\rho_{M_L}}\sqrt{\dfrac{D_G V_H}{D_L V_{\text{Rise}}}}}[We_{DH}]^{3/2} \times\left[\frac{V_{\text{Rise}}D_H}{D_G}\right]^{-1/2}\left[\frac{h_{Fe}}{D_H}\right]^1\left[\frac{V_H}{V_{\text{Rise}}}\right]^{1/2} \times\left[A[Re_{D_H}]^B f_1\left[\frac{\rho_L-\rho_V}{\rho_V}\right]f_2\left[\frac{h_L}{D_H}\right]f_3\left[\frac{A_H}{A_B}\right]\right]^{-3/2}, \quad (11a)$$

where, since we are assuming that the mass transfer is purely within the liquid-continuous region, we have

$$V_{\text{Rise}} = \frac{V_B}{1-\phi_{LC}} = \frac{V_B}{1-\phi_e}, \qquad We_{DH} = \frac{\rho_V V_H^2 D_H}{\sigma g_C},$$

and

$$Re_{DH} = \frac{\rho_V V_H D_H}{\mu_V}.$$

We have added the f_2 expression to allow a test on whether additional length scales are helpful. We have also added the f_3 expression to determine whether the mass transfer is dependent on the ratio of the total perforation area to the bubbling area of the tray in a manner not covered by its impact on hole velocity.

The Higbie theory suggests the indicated constants. We have, however, seen a complex dependency on the density ratio that may simply be due to the rigid relationships expected from the Higbie theory. We are using the Higbie theory to assist us only in identifying the appropriate dimensionless group candidates, not the specific functionality.

The data were regressed with the following format:

$$\frac{-\ln\left(1-\eta_{PT_{LC_{\text{only}}}}\right)}{6} = \frac{a_0}{1+m\dfrac{\rho_{M_V}}{\rho_{M_L}}\sqrt{\dfrac{D_G V_H}{D_L V_{\text{Rise}}}}(b_o[Re_L]^{b_1}[Sc_L]^{b_2})}[We_{DH}]^{a_1} \times[Re_{D_H}]^{a_2}\left[\frac{V_{\text{Rise}}D_H}{D_G}\right]^{a_3}\left[\frac{h_{Fe}}{D_H}\right]^{a_4}\left[\frac{V_H}{V_{\text{Rise}}}\right]^{a_5} \times\left[\frac{\rho_L-\rho_V}{\rho_V}\right]^{a_6}\left[\frac{h_L}{D_H}\right]^{a_7}\left[\frac{A_H}{A_B}\right]^{a_8}.$$

The resultant correlation for $\eta_{PT_{LC}}$ is therefore

$$\eta_{PT_{LC_{\text{only}}}} = 1-\exp \times\left(\frac{-6a_0}{1+m\dfrac{\rho_{M_V}}{\rho_{M_L}}\sqrt{\dfrac{D_G V_H}{D_L V_{\text{Rise}}}}(b_0[Re_L]^{b_1}[Sc_L]^{b_2})}[We_{DH}]^{a_1} \times[Re_{D_H}]^{a_2}\left[\frac{V_{\text{Rise}}D_H}{D_G}\right]^{a_3}\left[\frac{h_{Fe}}{D_H}\right]^{a_4}\left[\frac{V_H}{V_{\text{Rise}}}\right]^{a_5} \times\left[\frac{\rho_L-\rho_V}{\rho_V}\right]^{a_6}\left[\frac{h_L}{D_H}\right]^{a_7}\left[\frac{A_H}{A_B}\right]^{a_8}\right), \quad (11b)$$

where

$$Re_L = \frac{\rho_L V_{\text{Rise}} D_H}{\mu_L}, \qquad Sc_L = \frac{\mu_L}{\rho_L D_L}.$$

The inclusion of the liquid-phase Reynold's number and Schmidt number is made by analogy by turbulent heat transfer from a sphere where, if we use an identical approach as Higbie, successful heat-transfer correlations suggest that a liquid Reynolds number and Schmidt number dependency might exist. The vapor Schmidt number is not included in Eq. 11b since the variables that make up the vapor Schmidt number are already included in the correlation. After regression, the dimensionless groupings can be recast to isolate the resultant dependency on the vapor Schmidt number.

Using our subset of data, which excluded data sets expected to have either high entrainment or weeping, we regressed the data, and the resultant constants are

$$a_0 = 0.07099, \quad a_1 = -0.35829, \quad a_2 = 0.69800,$$
$$a_3 = -0.49332, \quad a_4 = 0.40320, \quad a_5 = 0.68085,$$
$$a_6 = -0.27800, \quad a_7 = 0.18597, \quad a_8 = 0.27914,$$
$$b_0 = 0.014, \quad b_1 = 0.4512, \quad b_2 = -0.08327.$$

(Constant Set A)

It is desirable to reduce the number of constants. Using the Higbie theory, Eq. 11a predicts that $b_0 = 1$, $b_1 = b_2 = 0$. We can determine whether a change from the prediction is justified by looking at the expression for R_{LC}:

$$R_{LC} = \frac{1}{1 + m\dfrac{\rho_{M_V}}{\rho_{M_L}}\sqrt{\dfrac{D_G V_H}{D_L V_{\text{Rise}}}}\,(b_0[Re_L]^{b_1}[Sc_L]^{b_2})}.$$

The importance of the liquid-side resistance is dependent on the nonunity term within the denominator. We can search for a different dependency on the liquid Reynolds number and liquid Schmidt number by calculating an "experimental" value for R_{LC}, assuming the experimental point efficiency is correct and using the values for a_0 through a_8. From this "experimental" value for R_{LC}, we can determine an "experimental" value for the nonunity term in the denominator of the expression for R_{LC}. We call this

$$m\frac{\rho_{M_V}}{\rho_{M_L}}\sqrt{\frac{D_G V_H}{D_L V_{\text{Rise Experimental}}}}$$

and normalize it by

$$m\frac{\rho_{M_V}}{\rho_{M_L}}\sqrt{\frac{D_G V_H}{D_L V_{\text{Rise}}}}.$$

In Figure 4a, this normalized value is plotted vs. the liquid Reynolds number. We see that the data surround unity, and there appears to be no statistical dependency of this ratio on the liquid Reynolds number. This is also true for the Schmidt number. For this reason, we recommend that we use for now $b_1 = b_2 = 0$.

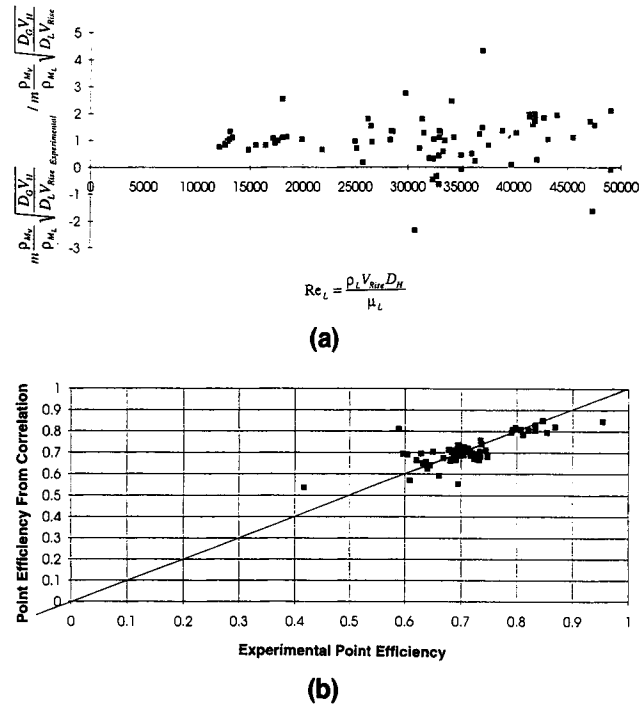

Figure 4. (a) Liquid-phase resistance parameter vs. liquid Reynolds number; (b) parity of selected point-efficiency data against low entrainment, low weeping correlation.

We can test the validity of the prediction that b_0 equals unity and our assumptions for contact times by selecting other values for b_0, and then reregressing on the constants a_0 through a_8. We have carried out this analysis, allowing b_0 to vary from 0.5 to 20. For this subset of data the average error of the correlation, for small values of b_0, is flat but increases when b_0 exceeds unity. As we have discussed, the value for b_0 has implications on the amount of the total resistance that is attributable to the liquid phase. For now, we will continue to utilize b_0 equal to unity, but will readdress this when we analyze the entire database.

If we use constants a_0 through a_8 and b_0 equal to unity, we can generate the parity plot, Figure 4b, for the subset of data used to generate this correlation. The average error is about 4.7% with 90% of the data within $\pm 10\%$.

Liquid continuous-only correlation for the entire database, considering entrainment

In Figures 5a and 5b we have plotted the ratio of the experimental point efficiency (calculated by ignoring entrainment) to the value estimated from Eq. 11b using Constant Set A and the entire database.

Figure 5a shows a decrease in the efficiency when $h_{2\phi}/T_S$ exceeds 1 or 2. This is not predicted by the current correlation. We attribute this falloff in efficiency to entrainment. Obviously, when the value for $h_{2\phi}/T_S$ exceeds unity, the physical meaning of $h_{2\phi}$ decreases. The ratio of froth height

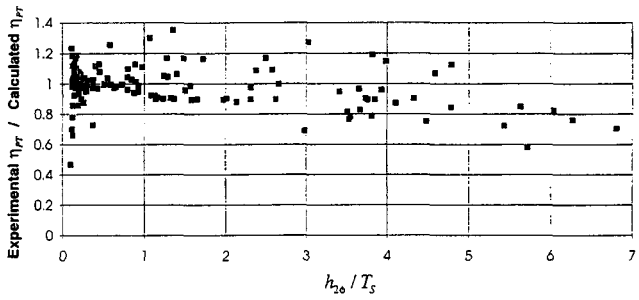

(a)

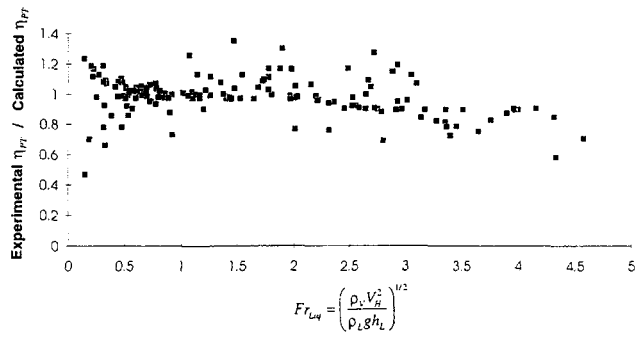

(b)

Figure 5. (a) Normalized efficiency vs. $h_{2\phi}/T_S$; (b) normalized efficiency vs. liquid Froude number.

$h_{2\phi}$, which is calculated as if there was no tray above, to the tray spacing is still, however, a reasonable grouping. For any value of $h_{2\phi}/T_S$, this calculated ratio is always a measure of the average upward kinetic energy of ejected droplets compared to the available vertical height. As this ratio increases, the number of droplets that can reach the tray above also increases, and the entrainment would be expected to increase.

In Figure 5b we plot the same ratio of efficiencies vs. the liquid Froude number. We had used a minimum value of about 0.5 to exclude data sets that may have significant weeping. Figure 5b supports this selected value. We also see a decrease in efficiency at large values of liquid Froude number. This decrease at large values results from entrainment since Bennett et al. (1995) show that increasing the hole velocity increases the froth height, which increases the entrainment.

Bennett et al. (1995) report that the normalized entrainment, E, behaves like

$$E\sqrt{\frac{\rho_V}{\rho_L}} = f\left(\frac{T_S}{h_{2\phi}}, \phi_{2\phi}\right).$$

Since entrainment is typically a secondary effect, we wish to look at a portion of the data that is well behaved but includes data sets with significant entrainment. The low vapor-density subset satisfies these criteria, and using the point efficiency correlation derived from the low entrainment subset of data we can back-calculate the entrainment values and correlate this vs. $T_S/h_{2\phi}$. This gives

$$E = 0.00335\left(\frac{T_S}{h_{2\phi}}\right)^{-1.10}\left(\frac{\rho_L}{\rho_V}\right)^{0.5}\phi_{2\phi}^{\beta}. \qquad (12)$$

For a system having a liquid-to-vapor density ratio comparable to that of air/water, this would give a value for entrainment of about 0.10 when $T_S/h_{2\phi}$ equals unity.

Dependency on the last two terms of Eq. 12 was assumed from the work of Bennett et al. (1995). Based on actual entrainment measurements for non-air/water systems, they suggest that

$$E = 0.04\left(\frac{T_S}{h_{2\phi}}\right)^{-1.04}\left(\frac{\rho_L}{\rho_V}\right)^{0.5}\phi_{2\phi}^{\beta}$$

gives reasonable values for entrainment, if $E \geq 0.1$, and overpredicted entrainment at lower values of entrainment.

Using Eq. 12, we can solve Eqs. 4b and 2 for the point efficiency that would result in the observed section efficiency. This is our first estimate of point efficiency that is on an entrainment-free basis. A regression of the entire database, assuming $b_0 = 1$, $b_1 = b_2 = 0$, yields the following values for a_0 through a_8;

$$a_0 = 0.00069, \quad a_1 = -0.09165, \quad a_2 = 0.43107,$$
$$a_3 = -0.01243, \quad a_4 = 0.43204, \quad a_5 = 0.16891,$$
$$a_6 = -0.04739, \quad a_7 = 0.51881, \quad a_8 = -0.32132,$$
$$\text{and} \quad b_0 = 1. \qquad \text{(Constant Set B)}$$

Figure 6 is a plot of the experimental data vs. those calculated with these new correlation parameters for the entire database. The average error is 6.3%, with 63% of the data within $\pm 5\%$, 83% of the data within $\pm 10\%$, and 95% of the data within $\pm 20\%$.

Testing the entrainment correlation

We have used the correlation for efficiency using Constant Set B to back-calculate the entrainment, which would give exact agreement with the correlation, and regressed on new powers, separately and together, for both $h_{2\phi}/T_S$ and ρ_L/ρ_V. When we resubstituted these new powers into our entrain-

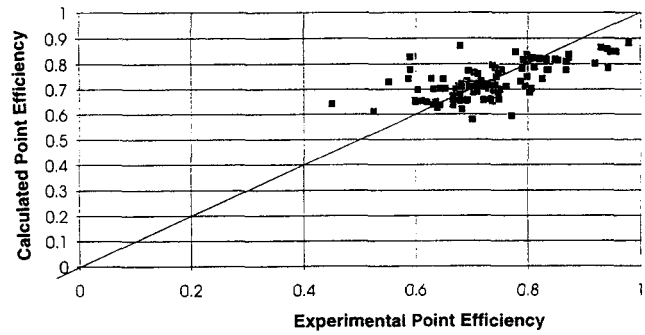

Figure 6. Parity of point-efficiency data against correlation values for entire database.

ment model and recalculated the constants a_0 through a_8, the resultant correlations increased the average error from a base of 6.3% to 8% to 13%. Since this is a significant increase in error, we decided to keep the original powers. We also analyzed the sensitivity to the coefficient 0.00335. We set the constant sequentially to 0.002, 0.006, and 0.01. We used these values for the coefficient to calculate the entrainment, then used these values of the entrainment to calculate new values of the point efficiency, and then calculated new values for constants a_0 through a_8. The resultant average errors were 7.53%, 10.3%, and 8.8%. Since we have obtained errors that are significantly larger than that obtained using the original coefficient, we choose the original value 0.00335.

Testing the liquid-phase resistance portion of the correlation

We have already seen that, within the scatter of the correlation, it is reasonable to expect that $b_1 = b_2 = 0$. The remaining coefficient that we need to address is the constant b_0. The value that we assume for b_0 will impact the average error of the correlation and will also have an impact on the fraction of the total resistance that is in the liquid phase. One method that has been used by others to estimate the liquid-phase resistance fraction is known as the slope-and-intercept method. It is described in Lockett (1986). This method requires that $\lambda = m/(L/V)$ vary throughout the test column and that the number of overall mass-transfer units be measured at several values of λ. An implicit assumption with this method is that the liquid- and vapor-side mass-transfer coefficients, despite the change in λ, are constant throughout the portion of the column where the mass transfer is being measured.

Figure 7a is a plot of the average error for the entire data set as a function of b_0. Zuiderweg (1982) reports that the slope-and-intercept method indicates that cyclohexane–*n*-heptane has about 50% of the resistance on the liquid side. In Figure 7b we have plotted the value for $1 - R_{LC}$ for a representative set of cyclohexane–*n*-heptane data within our composite database. The Zuiderweg estimate of the portion of the total mass transfer resistance for cyclohexane–*n*-heptane supports a value for b_0 equal to about 3, while minimizing the correlation error suggests $b_0 = 1$. If b_0 is chosen to be 2, the corresponding values for constants a_0 through a_8 are

$$a_0 = 0.00038, \quad a_1 = -0.07256, \quad a_2 = 0.5370,$$
$$a_3 = -0.06187, \quad a_4 = 0.47695, \quad a_5 = 0.07200,$$
$$a_6 = -0.06954, \quad a_7 = 0.59061, \quad a_8 = -0.40251,$$
$$\text{and} \quad b_0 = 2. \qquad \text{(Constant Set C)}$$

Values for b_0 other than unity can be reconciled with the Higbie theory by assuming different contact times. If we believe that the length scale is the same for both the liquid- and vapor-phase contact times, $b_0 = 2$ corresponds to

$$\frac{\theta_{L_{LC}}}{\theta_{G_{LC}}} = 4\frac{V_H}{V_{\text{Rise}}}.$$

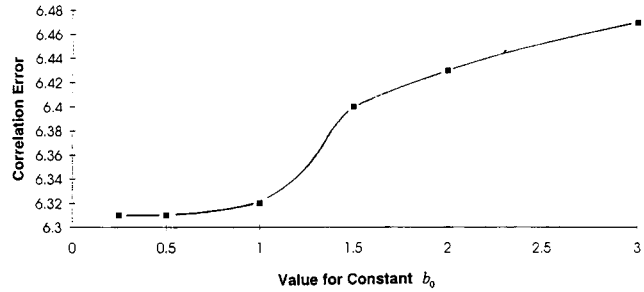

(a)

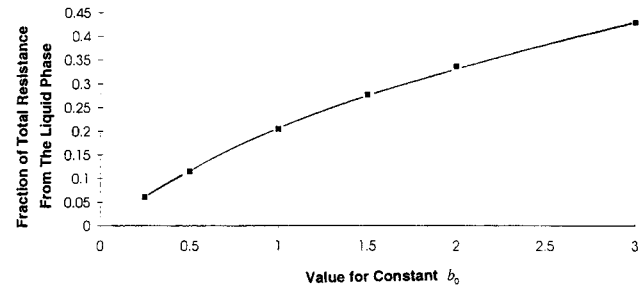

(b)

Figure 7. (a) Average error vs. value for constant b_0; (b) percent liquid-phase resistance vs. value for b_0.

Two mechanisms that could increase the ratio $\theta_{L_{LC}}/\theta_{G_{LC}}$ to values greater than V_H/V_{Rise} are vapor–liquid interface vibrations and liquid being dragged along with the bubble. Vibration is unlikely since it would tend to decrease the resistance on both the vapor and liquid side of the interface. Liquid being dragged along with the bubble is more likely. In this case, the upper bound for $\theta_{L_{LC}}$ is probably h_{Fe}/V_{Rise}. This would result in

$$\frac{\theta_{L_{LC}}}{\theta_{G_{LC}}} = \frac{V_H}{V_{\text{Rise}}}\frac{h_{Fe}}{D_B} \approx \frac{V_H}{V_{\text{Rise}}}\frac{h_{Fe}}{D_H},$$

which is $b_0 \approx 3$.

Based on data and mechanisms, we believe that b_0 is bounded by unity and 3. Due to the assumptions that are inherent to the slope-and-intercept method, the lack of a large number of such data for a variety of systems and operating conditions and the inherent difficulty in obtaining good-quality section efficiency data, it is premature to accept a value for b_0 that increases the overall error of our correlation. We recommend, therefore, that we keep $b_0 = 1$ and use Constant Set B.

Simplifying the liquid-continuous-only point-efficiency model

We can now use these constants, and by combining terms and neglecting those terms with very little impact, a simplified correlation can be obtained:

$$\eta_{PT_{LC_{only}}} = 1 - \exp\left[\frac{-0.0029}{1 + m\frac{\rho_{M_V}}{\rho_{M_L}}\sqrt{\frac{D_G(1-\phi_e)}{D_L(A_H/A_B)}}} \times \left(\frac{\rho_V V_H h_{Fe}}{\mu_V}\right)^{0.4136}\left(\frac{h_L}{D_H}\right)^{0.6074}\left(\frac{A_H}{A_B}\right)^{-0.3195}\right], \quad (13a)$$

and the average error is 6.41%. The parity plot is shown in Figure 8. When we had both the vapor Reynolds number and the dimensionless grouping $V_{\text{Rise}} D_H/D_G$, these expressions could be rearranged to yield both a dependency on Reynolds number and vapor Schmidt number. Since, as seen in Eq. 13a, a dependency on $V_{\text{Rise}} D_H/D_G$ is no longer needed for a successful correlation, this implies that the vapor-phase Schmidt number is not important for the vapor-phase resistance. This is surprising. Our database did include a change in the vapor-phase Schmidt number of about a factor of 2. As a final check, we added Sc_V to Eq. 13a as an additional correlation parameter. Our reregression gave a power on Sc_V of -0.002. Our conclusion is that no vapor Schmidt number dependency is required for our database.

If we were to use $b_0 = 2$, we would get,

$$\eta_{PT_{LC_{only}}} = 1 - \exp\left[\frac{-0.000384}{1 + 2m\frac{\rho_{M_V}}{\rho_{M_L}}\sqrt{\frac{D_G(1-\phi_e)}{D_L(A_H/A_B)}}} \times \left(\frac{\rho_V V_H h_{Fe}}{\mu_V}\right)^{0.5408}\left(\frac{h_L}{D_H}\right)^{0.7880}\left(\frac{A_H}{A_B}\right)^{-0.5296}\right], \quad (13b)$$

and the average error is 6.95%.

A Model Addressing Both the Vapor- and Liquid-continuous Regions

In our liquid-continuous-only model, we assumed that all of the mass was contained within the liquid-continuous region, which was assumed to have a height h_{Fe}. We can move from a liquid-continuous-only model to a two-zone model by accounting for the mass that is contained within the vapor-continuous region. This results in the liquid-continuous froth density decreasing from ϕ_e to ϕ_{LC}, and the liquid inventory within the liquid continuous region decreasing from all the liquid, h_L, which equals $h_{Fe}\phi_e$, to $h_{Fe}\phi_{LC}$. The result is that the efficiency within the liquid-continuous region decreases. We would expect, therefore, that the point efficiency for the liquid-continuous region is

$$\eta_{PT_{LC}} = 1 - \exp\left[\frac{-0.0029}{1 + m\frac{\rho_{M_V}}{\rho_{M_L}}\sqrt{\frac{D_G(1-\phi_{LC})}{D_L(A_H/A_B)}}} \times \left(\frac{\rho_V V_H h_{Fe}}{\mu_V}\right)^{0.4136}\left(\frac{h_{Fe}\phi_{LC}}{D_H}\right)^{0.6074}\left(\frac{A_H}{A_B}\right)^{-0.3195}\right]. \quad (14a)$$

Based on the Higbie theory, as applied to the vapor-continuous region, we have:

$$\eta_{PT_{VC}} = 1 - \exp\left[\frac{-C_{VC}}{K_S\left[1 + m\frac{\rho_{M_V}}{\rho_{M_L}}\sqrt{\frac{D_G}{D_L}\frac{(h_{2\phi} - h_{Fe})}{D_P}}\right]} \times \sqrt{\frac{D_G V_{ej}}{\pi D_P}\frac{\rho_V}{\rho_L - \rho_V}}\frac{h_{2\phi} - h_{Fe}}{D_P}\phi_{VC}\right]. \quad (14b)$$

If our choice of contact times and the critical Weber number are correct, $C_{VC} = 12$. To calculate the liquid-resistance contact time, we have used the initial vertical velocity of the droplet, V_{ej}, rather than an average value, which is $0.5V_{ej}$ (if drag is neglected). For the vapor-phase resistance, we have again chosen V_{ej} to calculate the vapor-resistance contact time, and it would be more correct to use the average relative velocity, $|0.5V_{ej} - V_B|$. Finally, we also used a critical Weber number of 15 to determine the size of the droplet. Although this is probably a reasonable estimate of the largest droplet diameter, we are actually interested in an average droplet size. Although we might expect a value for C_{VC} of 12 if we used the more complex expressions for relative velocity, the average velocity of the drop, and the critical Weber number, including this detail complicates the correlation, and we have chosen to determine the value for C_{VC} from the data.

In addition to C_{VC}, the only other unknowns in the previous equation are ϕ_{LC} and ϕ_{VC}, but they are related to the fraction of the total bi-phase mass, which is contained in the vapor-continuous region, f, by

$$\phi_{VC} = \frac{\phi_e h_{Fe}}{(h_{2\phi} - h_{Fe})} f$$

$$\phi_{LC} = \phi_e(1 - f).$$

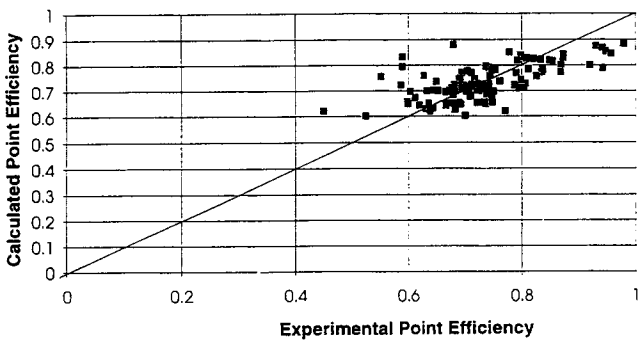

Figure 8. Parity of experimental point efficiency against the liquid-continuous-only correlation.

In addition

$$\eta_{PT} = \eta_{PT_{VC}} + \eta_{PT_{LC}}(1 - \eta_{PT_{VC}}).$$

Both C_{VC} and f need to be calculated. One approach is to calculate the best overall value for C_{VC} and determine f for each data point. We found that the existence of a nonzero solution for $f \leq 1$ was strongly dependent on the chosen value for C_{VC}. Even when a solution for $f \leq 1$ was obtained, the calculated value for f was often very sensitive to the chosen value for C_{VC}, for example, a 3% variation in C_{VC} gave a 20% variation in f. With such a sensitivity, the approach of determining f for each data set and developing an overall equation for f will not be successful.

We know from the work of Bennett et al. (1995) that the biphase becomes predominantly liquid continuous as h_L/D_H increases. We would expect that the fraction of the total liquid in the vapor-continuous region goes to zero as h_L/D_H increases. In addition, as h_L/D_H approaches zero, the biphase becomes completely vapor continuous, and ϕ_{VC} should approach ϕ_{LC} and both should approach $h_L/h_{2\phi}$. An equation that has this functionality is

$$f = \left(1 - \frac{h_{Fe}}{h_{2\phi}}\right) e^{-C_1(h_L/D_H)}. \tag{15}$$

In Figure 9 we show the results from a parametric study that gives for our composite database the average error as a function of C_{VC} for a number of constant C_1-lines. For all cases, we see the average error increasing from that obtained from the liquid-continuous-only correlation. A value of $C_1 = 0.10$ corresponds to an average value of f of about 0.5 for our entire database. Data reported by Hofhuis and Zuiderweg (1979) in their figure 5 present air/water froth density profiles that yield values for f of about 0.5 over a range of vapor rates. Based on their result, we will assume that $C_1 = 0.10$. For this value of C_1, the average error becomes minimum at $C_{VC} = 3.2$ at 13.25%. For this case, and using the entire database (where the average value for η_{PT} is 73%), the average value for $\eta_{PT_{LC}}$ is 68.5%. Since the average value of $\eta_{PT_{LC}}$ is 94% of the average value of η_{PT}, for our database, most of the mass transfer occurs within the liquid-continuous region. Since the tray spacing is typically four times larger than the height of the liquid-continuous region, our assumption that the tray spacing has little impact on point efficiency is reasonable.

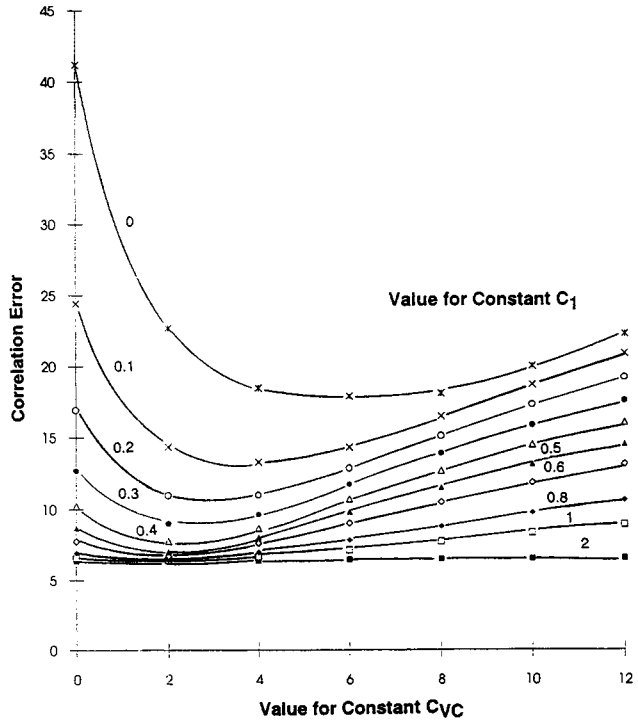

Figure 9. Sensitivity of two-zone correlation error on values for constants C_{VC} and C_1.

Correlation Recommendation

We have investigated the contribution of mass transfer within the vapor-continuous region to the total mass transfer. Although the vapor-continuous portion may at times be significant, our liquid-continuous-only model is still the most successful correlation. Equations 14a, 14b, and 15 should therefore only be used if a separation of the mass transfer within the vapor-continuous and liquid-continuous regions is needed. When the overall point efficiency is needed, we recommend that the following correlation be used for the point efficiency:

$$\eta_{PT_{LC_{only}}} = 1 - \exp\left[\frac{-0.0029}{1 + m\frac{\rho_{M_V}}{\rho_{M_L}}\sqrt{\frac{D_G(1-\phi_e)}{D_L(A_H/A_B)}}} \times \left(\frac{\rho_V V_H h_{Fe}}{\mu_V}\right)^{0.4136}\left(\frac{h_L}{D_H}\right)^{0.6074}\left(\frac{A_H}{A_B}\right)^{-0.3195}\right]. \tag{13a}$$

Figures 10a, 10b and 10c are plots of all of the point-efficiency data (corrected by using Eq. 12 for entrainment) normalized by values predicted from Eq. 13a. These normalized values are plotted vs. $h_{2\phi}/T_S$ in Figure 10a and ρ_L/ρ_V in Figure 10b. These figures show that Eq. 12 does a reasonable job in predicting the changes in entrainment due to changes in $h_{2\phi}/T_S$ and ρ_L/ρ_V.

In Figure 10c we have also plotted the normalized point-efficiency data vs. the liquid Froude number, which has shown to be successful in correlating weeping. We find that Eq. 13a is valid throughout almost the entire range of the liquid Froude number, with the possible exception of a few sets of data with lower efficiency values when the liquid Froude number is less than 0.4.

Calculating Tray Efficiency: Entrainment, Weeping, Flow Direction, and Tray Mixing

We recommend that the point efficiency be calculated from the liquid-continuous-only model, Eq. 13a,

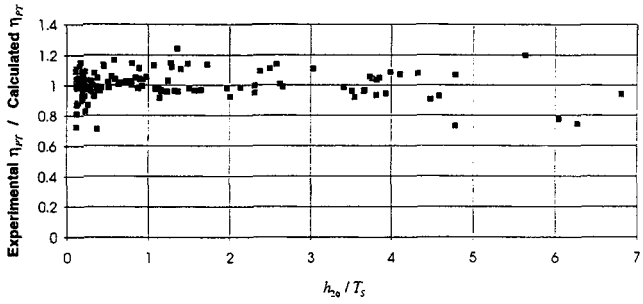

(a)

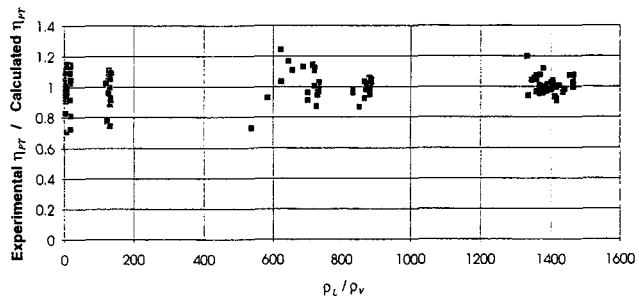

(b)

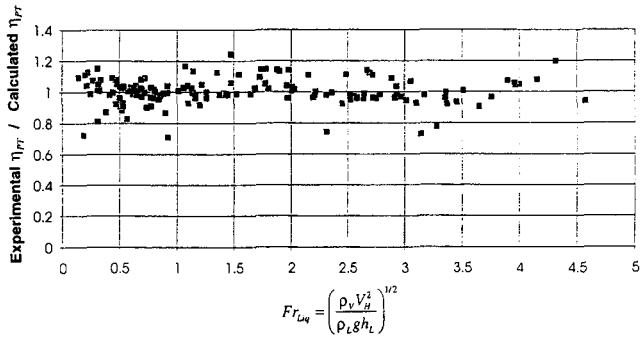

(c)

Figure 10. Normalized point efficiency vs.: (a) $h_{2\phi}/T_S$ for the entire database; (b) ρ_L/ρ_V for the entire database; (c) liquid Froude number for the entire database.

$$\eta_{PT_{LC_{only}}} = 1 - \exp\left[\frac{-0.0029}{1 + m\frac{\rho_{M_V}}{\rho_{M_L}}\sqrt{\frac{D_G(1-\phi_e)}{D_L(A_H/A_B)}}} \times \left(\frac{\rho_V V_H h_{Fe}}{\mu_V}\right)^{0.4136}\left(\frac{h_L}{D_H}\right)^{0.6074}\left(\frac{A_H}{A_B}\right)^{-0.3195}\right]. \quad (13a)$$

This model is tested for values of h_L/D_H greater than about unity. This covers typical ranges for frothlike flow and many cases for spraylike flow. The application of the correlation to conditions that are heavily spraylike, for example, when h_L/D_H is less than about unity, is untested.

The degree of vapor mixing can be estimated from Katayama and Imoto (1972), who report that the vapor can be considered unmixed if the vapor Peclet number, $Pe_G \geq 50$, where

$$Pe_G = \frac{V_B Z^2}{De_G(T_S - h_{2\phi})}.$$

Lockett (1986) recommends on page 171 that a value for $De_G = 0.01$ m^2/s be used. If $h_{2\phi}/T_S \geq 1$, the vapor should be considered unmixed.

When the vapor is well mixed but the liquid is partially mixed, we have verified that the numerical solution for the Murphree efficiency, for the ranges of $0.5 \leq \lambda \leq 3.0$, $0.4 \leq \eta_{PT} \leq 1.0$, and $0 \leq Pe_L \leq 1{,}000$, can be approximated to within an average error of $\pm 0.4\%$ by

$$\eta_{MW_{\text{vapor-mixed}}} = \frac{[1 + (\lambda\eta_{PT}/N)]^N - 1}{\lambda}. \quad (3a)$$

Since the vapor is assumed to be mixed prior to entering the tray above, there is no dependency of the Murphree efficiency on the liquid flow direction (parallel or crossflow).

When the vapor is unmixed, the Murphree efficiency is dependent upon the flow direction. For parallel flow we have found that the Diener solution, for the ranges of $0.5 \leq \lambda \leq 3.0$, $0.4 \leq \eta_{PT} \leq 1.0$, and $0 \leq Pe_L \leq 1{,}000$, can be approximated to within an average error of $\pm 1.5\%$ by

$$\eta_{MV_{\text{Parallel,unmixed-vapor}}} = \frac{[1 + (\lambda\eta_{PT}/N)]^N - 1}{\lambda} \times [1 + 0.0463\lambda^{0.6255}\eta_{PT}^{1.69591}Pe_L^{0.16625}]. \quad (4a)$$

For the cross-flow case, the Diener solution for the ranges of $0.5 \leq \lambda \leq 3.0$, $0.4 \leq \eta_{PT} \leq 1.0$, and $0 \leq Pe_L \leq 1{,}000$ can be approximated to within an average error of $\pm 1.5\%$ by

$$\eta_{MV_{\text{Cross-flow, unmixed-vapor}}} = \frac{[1 + (\lambda\eta_{PT}/N)]^N - 1}{\lambda} \times [1 - 0.0335\lambda^{1.07272}\eta_{PT}^{2.51844}Pe_L^{0.17524}], \quad (4b)$$

where N is dependent on the liquid Peclet number:

$$N = \frac{Pe_L + 2}{2} \quad (3b)$$

and

$$Pe_L = \frac{q_L Z^2}{A_B h_L De_L}.$$

We recommend that the liquid eddy diffusivity be determined from the correlation of Bennett and Grimm (1991) for rectangular trays, but multiplied by four to compensate for the inlet maldistribution and tray curvature typical of actual tray design. Therefore

$$De_L = 4(0.024)\left[gh_{2\phi}^3\right]^{1/2}.$$

Equations 3a, 4a, and 4b neglect weeping and entrainment. Our composite database has not shown a decrease in performance associated with weeping as long as the liquid Froude number is greater than 0.5, where

$$Fr_{\text{Liq}} = \left(\frac{\rho_V V_H^2}{\rho_L g h_L}\right)^{1/2}.$$

The entrainment can be estimated from Eq. 12:

$$E = 0.00335\left(\frac{T_S}{h_{2\phi}}\right)^{-1.10}\left(\frac{\rho_L}{\rho_V}\right)^{0.5}\phi_{2\phi}^{\beta}, \tag{12}$$

where, $\phi_{2\phi} = h_L/h_{2\phi}$ and

$$\beta = 0.5\left(1-\tanh\left[1.3\ln\left(\frac{h_L}{D_H}\right)-0.15\right]\right)$$

and h_L is obtained from Bennett et al. (1983):

$$h_L = h_{Fe}\phi_e$$

$$h_{Fe} = h_W + C\left(\frac{Q_L}{\phi_e}\right)^{2/3}$$

$$\phi_e = \exp(-12.55K_S^{0.91}),$$

where K_S is the density corrected vapor velocity over the bubbling area, expressed in m/s, and C is a constant:

$$C = 0.501 + 0.439\exp(-137.8h_W)$$

and the weir height h_W is expressed in meters.

The overall height of the froth, $h_{2\phi}$, is obtained from Bennett et al. (1995):

$$\frac{h_{2\phi}}{h_{Fe}} = 1 + \left[1+6.9\left(\frac{h_L}{D_H}\right)^{-1.85}\right]\frac{Fr_V}{2},$$

where

$$Fr_V = \frac{V_{ej}^2}{gh_{Fe}}$$

and

$$V_{ej} = 3K_S\sqrt{\frac{\sqrt{3}}{(A_H/A_B)\phi_e}}.$$

The calculated value for $h_{2\phi}$ should still be used even if the value is greater than T_S.

The value of the entrainment can be used to calculate the Murphree efficiency, accounting for the recirculation resulting from entrainment from

$$\frac{\eta_{MV}(E)}{\eta_{MV}(E=0)} = 1 - 0.8\eta_{PT}\lambda^{0.543}E\frac{V}{L}, \tag{2}$$

where $\eta_{MV}(E=0)$ is calculated from Eq. 3a, 4a, or 4b, depending on the vapor and liquid mixing and flow direction, and η_{PT} is calculated from Eq. 13a. The section efficiency is now calculated from

$$\eta_{\text{SECT}} = \frac{\ln(1+\eta_{MV}(\lambda-1))}{\ln\lambda}, \tag{1}$$

where $\eta_{MV} = \eta_{MV}(E)$.

Notation

D = molecular diffusivity
De = eddy diffusivity
g = acceleration due to gravity
g_C = constant that may be required for Newton's law
q_L = volumetric flow rate of liquid onto tray
T_S = tray spacing
Z = flow path of tray
β = power on $\phi_{2\phi}$ in entrainment correlation
ρ = mass density
σ = surface tension
μ = molecular viscosity

Literature Cited

AIChE Research Committee, *Bubble Tray Design Manual*, AIChE (1958).

Bennett, D. L., R. Agrawal, and P. J. Cook, "New Pressure Drop Correlation for Sieve Tray Distillation Columns," *AIChE J.*, **29**, 434 (1983).

Bennett, D. L., and H. J. Grimm, "Eddy Diffusivity for Distillation Sieve Trays," *AIChE J.*, **37**, 589 (1991).

Bennett, D. L., and K. A. Ludwig, "Understand the Limitations of Air/Water Testing of Distillation Equipment," *Chem. Eng. Prog.*, **90**, 4 (1994).

Bennett, D. L., A. S. Kao, and L. W. Wong, "A Mechanistic Analysis of Sieve Tray Froth Height and Entrainment," *AIChE J.*, **41**, 2067 (1995).

Biddulph, M. W., and M. M. Dribika, "Distillation Efficiencies on a Large Sieve Plate with Small-diameter Holes," *AIChE J.*, **32**(8), 1383 (1986).

Chan, H., and J. R. Fair, "Prediction of Point Efficiencies on Sieve Trays," *Ind. Eng. Chem. Process Des. Dev.*, **23**, 814 (1984).

Diener, D. A., "Calculation of Effect of Vapor Mixing on Tray Efficiency," *Ind. Eng. Chem. Process Design Dev.*, **6**, 499 (1967).

Fair, J. R., "How to Predict Sieve Tray Entrainment and Flooding," *Petro/Chem. Eng.*, **33**(10), 45 (1961).

Gautreaux, M. E., and H. E. O'Connell, "Effect of Length of Liquid Path on Plate Efficiency," *Chem. Eng. Prog.*, **51**(5), 232 (1955).

Higbie, R., "The Rate of Adsorption of a Pure Gas into a Still Liquid during Short Periods of Exposure," *Trans. AIChE*, **31**, 365 (1935).

Hughmark, G. A., "Point Efficiencies for Tray Distillations," *Chem. Eng. Prog.*, **61**, 97 (1965).

Hofhuis, P. A. M., and F. J. Zuiderweg, "Sieve Plates: Dispersion Density and Flow Regimes," *AIChE Symp. Ser.*, **56**, 2.2/1 (1979).

Jones, J. B., and C. Pyle, "Relative Performance of Sieve and Bubble-Cap Plates," *Chem. Eng. Prog.*, **51**, 424 (1955).

Katayama, H., and T. Imoto, "Effect of Vapor Mixing on the Tray Efficiency of Distillation Columns," *J. Chem. Soc. Japan*, **9**, 1745 (1972).

Kumar, A., T. E. Degaleeson, G. S. Ladda, and H. E. Hoelscher, "Bubble Swarm Characteristics in Bubble Columns," *Can. J. Chem. Eng.*, **54**, 503 (1976).
Lockett, M. J., and S. Banik, "Weeping from Sieve Trays," AIChE Meeting, San Francisco (1984).
Lockett, M. J., *Distillation Tray Fundamentals*, Cambridge Univ. Press, New York (1986).
Nutter, D. E., "Ammonia Stripping Efficiency Studies," *AIChE Symp. Ser.*, **68**, 73 (1971).
Prado, M., and J. R. Fair, "Fundamental Model for the Prediction of Sieve Tray Efficiency," *Ind. Eng. Chem. Res.*, **29**, 1031 (1990).
Sakata, M., and T. Yanagi, "Performance of a Commercial Scale Sieve Tray," *AIChE Symp. Ser.*, **56**, 3.2/21 (1979).
Soulders, M., and G. G. Brown, "Design of Fractionating Columns," *Ind. Eng. Chem.*, **26**, 98 (1934).
Treybal, R. E., *Mass Transfer Operations*, 2nd ed., McGraw-Hill, New York (1968).
Yanagi, T., and M. Sakata, "Performance of a Commercial Scale Fourteen Percent Hole Area Sieve Tray," *Ind. Eng. Chem. Process Des. Dev.*, **21**, 712 (1982).
Zuiderweg, F. J., "Sieve Trays: A View on the State of the Art," *Chem. Eng. Sci.*, **37**, 1441 (1982).

Manuscript received Apr. 1, 1996, and revision received Jan. 10, 1997.